Nusantara Hasana Journal
Volume 3 No. 7 (Desember 2023), Page: 236-248
E-ISSN : 2798-1428

HYDROLOGICAL EXTREMES AND WATER ALLOCATION IN TROPICAL RIVER BASINS: EVIDENCE FROM THE JENEBERANG RIVER, MAKASSAR

Abd Rakhim Nanda

Universitas Muhammadiyah Makassar, Indonesia

***Email: abd.rakhimnanda@unismuh.ac.id**

Abstract
This study proposes an adaptive water allocation framework based on the pipeline P(t)→SPI(t)→A(t), with SPI serving as a control variable to represent hydrological conditions probabilistically. Analysis shows that rainfall is non-stationary and dominated by stochastic variability, making a mean-based approach unrepresentative. Integrating SPI enables dynamic adjustment of allocations to actual conditions, reducing the deficit by 12.96% and increasing efficiency from 46.32% to 53.49%. Validation of the dataset shows high consistency with the presence of systematic scale bias, making it more suitable for anomaly-based analysis. Sensitivity analysis identifies bounded responsiveness, where the system is adaptive under normal conditions but remains stable under extreme conditions. Conceptually, this study transforms the SPI into a decision variable, thereby establishing a causal relationship between hydroclimatic variability and allocation decisions and enhancing the system's resilience to drought risk.
Keywords: *Adaptive water allocation, Standardized Precipitation Index, Hydrological drought, Non- stationary hydrology*

INTRODUCTION

Tropical hydroclimatic variability is inherently fluctuating, unstable, and non-stationary, implying that water availability cannot be treated as a constant state variable but must instead be modeled as a dynamically evolving stochastic process (Shao et al., 2022). This intrinsic variability substantially amplifies supply uncertainty and increases the likelihood of allocation failure, particularly under drought conditions. Furthermore, drought response is intrinsically complex, as meteorological drought does not propagate linearly into agricultural drought; rather, the transformation is mediated by climate regimes, vegetation characteristics, and soil-water interactions, leading to heterogeneous impacts across spatial domains (Sun et al., 2023). Within the Jeneberang watershed, irregular precipitation patterns interact with relatively inelastic cross-sectoral water demands, generating persistent supply-demand mismatches. In addition, drought propagation is strongly influenced by irrigation systems, groundwater buffering capacity, and infrastructural constraints, indicating that allocation strategies must explicitly incorporate the coupled dynamics between hydrological states and sectoral water requirements (Fawen et al., 2023).

A critical limitation emerges from the dominance of deterministic and static allocation models that rely on mean hydrological conditions as their primary assumption. Such formulations are structurally inadequate for representing tropical systems characterized by non-stationarity, non-linearity, and temporal variability

Nusantara Hasana Journal
Volume 3 No. 7 (Desember 2023), Page: 236-248
E-ISSN : 2798-1428

(Wu et al., 2020). The sensitivity of river discharge to climate variability and drought further highlights the responsiveness of fluvial systems to hydroclimatic forcing, reinforcing the inadequacy of static representations (Noorisameleh et al., 2020). Consequently, these models fail to capture the functional interdependence between rainfall variability, drought intensity, and allocation decisions, leading to non-adaptive and inefficient allocation outcomes. Although datasets such as CHIRPS and NASA POWER enhance the spatio-temporal representation of precipitation, their application remains largely descriptive rather than operational. Similarly, SPI(t) is predominantly utilized as a monitoring indicator, rather than being embedded as an endogenous control variable within allocation frameworks. This limitation is particularly critical, as future drought assessment requires indicators that are directly coupled with adaptive management responses (Tramblay et al., 2020). The absence of such integration reveals a structural disconnect between hydrological information and operational decision-making processes.

From a methodological standpoint, existing allocation approaches still treat water availability as a fixed parameter, thereby failing to represent the stochastic, non-linear, and temporally evolving nature of hydrological processes. The increasing complexity of drought propagation under global warming conditions demonstrates that hydrological responses are governed by interacting dynamic processes rather than static relationships (Zhang et al., 2022). Moreover, the adoption of non-stationary modeling frameworks is essential, as hydrological drought is influenced by both climate variability and anthropogenic activities (Jehanzaib et al., 2020). In response to these limitations, this study reformulates SPI(t) from a purely diagnostic indicator into a control variable through a causal analytical pipeline, $P(t) - SPI(t) - A(t)$, thereby explicitly linking precipitation dynamics, drought states, and allocation decisions. The primary contribution of this research lies in redefining SPI(t) as a decision variable that operationally bridges hydrological conditions and water distribution policies. Methodologically, the proposed framework integrates time-series analysis, probabilistic transformation, and allocation optimization; practically, it enables adaptive allocation strategies that dynamically respond to drought conditions, thereby improving allocation efficiency and reducing deficit risk. This research is illustrated in Figure 1.

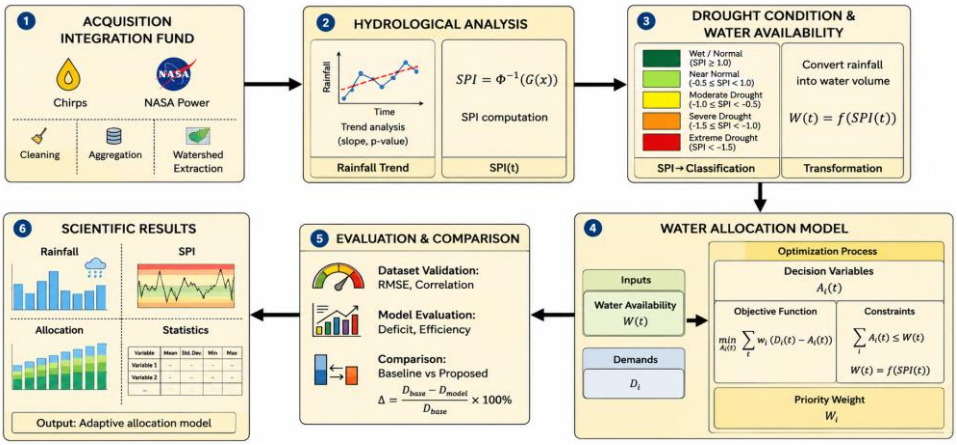

Figure 1. Integrated Hydrological Analysis and SPI-Based Water Allocation Framework

Nusantara Hasana Journal
Volume 3 No. 7 (Desember 2023), Page: 236-248
E-ISSN : 2798-1428

METODE

Data Collection

The drought index functions as an operational signal translating hydroclimatic states into decision variables (Sun et al., 2022), such that $A_i(t)$is optimized conditional on $W(t)$to minimize deficit under supply-demand bounds. Hence, hydrological conditions are endogenized within the allocation mechanism. Empirical validation and baseline comparison confirm that efficiency gains arise from adaptive responsiveness, whereby allocation is rigorously expressed as a non-stationary dynamic function rather than a static historical mean representation (Guillory et al., 2023).

Table 1. Dataset specification used in the study

Dataset	Source	Temporal Resolution	Spatial Resolution	Variable	Role
CHIRPS v3.0	Satellite	Monthly	0.05°	Precipitation	Primary dataset
NASA POWER	Satellite	Daily-Monthly	Point-based	PRECTOTCORR	Validation dataset

Hydrological Modelling and Optimization

The modelling framework is formulated as an inferential pipeline that transforms multi-source precipitation into allocation decision variables by integrating statistical transformations and explicit mathematical optimisation. Given that meteorological-hydrological drought linkages are inherently temporal and cross-scale, precipitation indicators are first converted into operational hydrological variables prior to entering the decision model (Li et al., 2020). Subsequently, an integrated understanding of drought characteristics, propagation mechanisms, and governing factors enables the translation of hydrological indicators into adaptive allocation responses, ensuring that optimization reflects dynamic hydroclimatic conditions rather than static assumptions (Raposo et al., 2023).

Data Pre-processing

The pre-processing stage ensures statistical consistency through imputation, anomaly detection, and temporal aggregation for multi-source alignment. Standardization is defined as:

$$Z = \frac{X - \mu}{\sigma}$$

Enforces normalization, stabilizes distribution fitting, and reduces magnitude-induced bias, producing a structured precipitation time series $P(t)$for subsequent probabilistic inference and optimization.

Drought Index Computation (SPI)

The drought index is computed via a probabilistic transformation using the Gamma distribution, subsequently mapped into the standard normal distribution to ensure temporal comparability. Index-based approaches are effective in reducing drought complexity into a consistent quantitative metric (Yang et al., 2023). The formulation is given:

Nusantara Hasana Journal
Volume 3 No. 7 (Desember 2023), Page: 236-248
E-ISSN : 2798-1428

$$SPI = \Phi^{-1}(G(x))$$

Employs the inverse standard normal function Φ^{-1}, producing a standardized $SPI(t)$that enables quantitative anomaly detection in precipitation.

Drought State Classification

The standardized $SPI(t)$ is discretized into four hydrological regimes to capture drought dynamics, as risk is governed by both intensity and temporal transitions (Dai et al., 2020)

$$S(t) = \begin{cases} \text{Wet / Normal}, & SPI(t) \geq 0 \\ \text{Near Normal}, & -0.5 \leq SPI(t) < 0 \\ \text{Moderate Drought}, & -1.0 \leq SPI(t) < -0.5 \\ \text{Severe Drought}, & SPI(t) < -1.0 \end{cases}$$

Dynamic Water Availability and Allocation Optimization

Dynamic availability is derived via a monotonic transformation of $SPI(t)$, translating meteorological drought into operational supply signals (Guo et al., 2020)

$$W(t) = W_{\max} \cdot \left(\frac{SPI(t) - SPI_{\min}}{SPI_{\max} - SPI_{\min}}\right)$$

Maps hydrological deterioration directly into reduced $W(t)$, where W_{max} denotes system capacity and SPI_{min}, SPI_{max} bound observed conditions. Allocation is formulated as constrained deficit minimization, incorporating dynamic supply (Dai et al., 2022)

$$\min_{A_i(t)} \sum_{i=1}^{n} w_i \left(D_i(t) - A_i(t)\right)$$

$$\sum_{i=1}^{n} A_i\,(t) \leq W(t)$$

The constraint enforces feasibility under evolving availability, while $W(t) = f(SPI(t))$ endogenizes hydrological states, enabling adaptive, non-stationary allocation driven by real-time drought conditions.

RESULTS AND DISCUSSION

Rainfall Trend Analysis

Rainfall dynamics in the Jeneberang watershed are evaluated using the Mann-Kendall test and Sen's slope estimator due to their robustness to outliers and suitability for non-stationary series. Figure 2 presents the P(t) time series, revealing pronounced interannual variability and strong seasonality, yet no statistically consistent long-term trend.

Nusantara Hasana Journal
Volume 3 No. 7 (Desember 2023), Page: 236-248
E-ISSN : 2798-1428

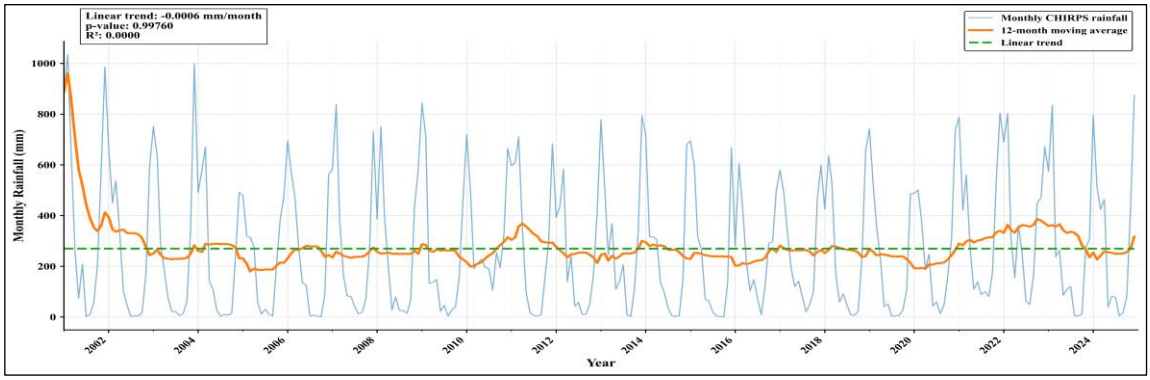

Figure 2. Monthly rainfall time series and Sen's slope trend in the Jeneberang watershed

Figure 2 indicates that rainfall variability dominates over any long-term trend, necessitating statistical validation. Quantitative results are summarized in Table 2 using Sen's slope and the Mann-Kendall test.

Table 2. Rainfall trend analysis using Mann-Kendall and Sen's slope

Parameter	Value	Interpretation
Observation Period	2001-2024	Analysis timeframe
Number of Observations	288 months	Time series length
Mean Rainfall	269.75 mm/month	Climatological average
Standard Deviation	257.09 mm/month	High variability
Minimum	0.95 mm/month	Extremely dry condition
Maximum	1035.06 mm/month	Extremely wet condition
Sen's Slope	-0.0072 mm/year	Very weak decreasing trend
p-value (Mann-Kendall)	0.99760	Not significant ($p \geq 0.05$)

Based on Table 2, the Sen's slope (-0.0072 mm/year) and p-value (0.99760 > 0.05) confirm that rainfall trends are statistically insignificant. The high standard deviation relative to the mean indicates that temporal variability dominates over deterministic patterns. Analytically, this condition renders mean-based estimation of W(t) unreliable, particularly under extreme events. Therefore, Figure 2 and Table 2 collectively demonstrate that rainfall in the Jeneberang watershed is stochastic, necessitating an adaptive allocation framework driven by real-time hydrological conditions.

SPI-Based Drought Characterization

Drought is probabilistically characterized using $SPI(t)$derived from precipitation time series, as rainfall-based indices effectively capture drought dynamics when linked to system hydrological responses (Wang et al., 2020). Accordingly, hydrological conditions are not represented by mean values alone but by their probability distribution, event frequency, and persistence of extremes. Figure 3(a) illustrates the temporal evolution of SPI(t), while Figure 3(b) presents its probabilistic distribution.

Nusantara Hasana Journal
Volume 3 No. 7 (Desember 2023), Page: 236-248
E-ISSN : 2798-1428

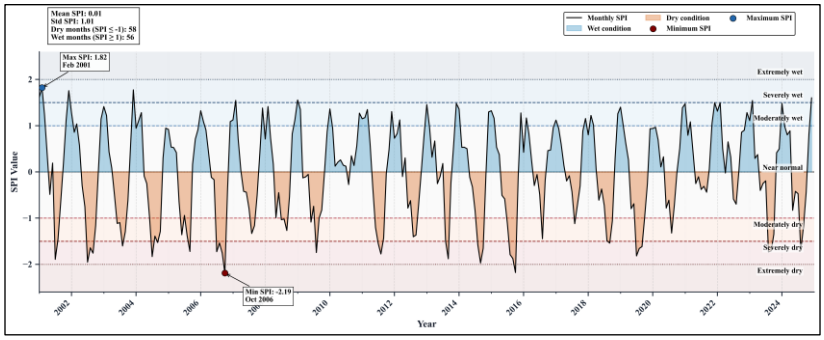

3(a)

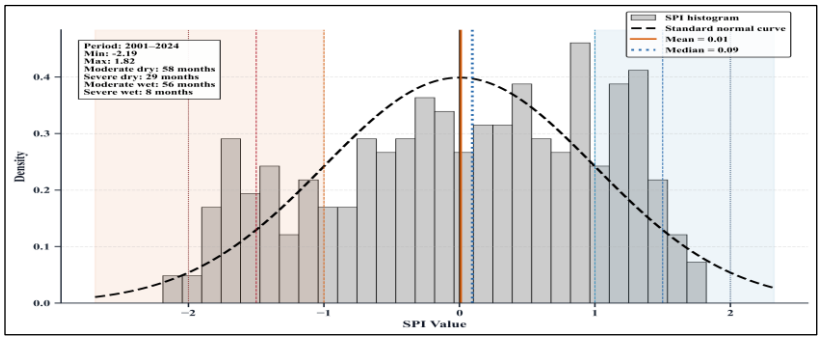

3(b)

Figure 3. (a) Temporal dynamics of SPI and (b) probabilistic distribution of SPI values in the Jeneberang watershed

Figure 3(a) shows that SPI(t) exhibits high variability, with rapid transitions between wet and dry states, and lacks a consistent long-term trend, indicating the dominance of stochastic hydrological dynamics. Figure 3(b) reveals a distribution concentrated around near-normal conditions with observable tail behavior, indicating the presence of hydrological extremes. The frequency of occurrence across SPI-based categories is summarized in Table 3.

Table 3. Frequency of hydrological conditions based on SPI categories

Category	Definisi SPI	Jumlah	Persentase
Normal/Wet	SPI ≥ 0	152 bulan	52.78%
Near Normal	-0.5 ≤ SPI < 0	48 bulan	16.67%
Moderate Drought	-1.0 ≤ SPI < -0.5	30 bulan	10.42%
Severe Drought	SPI < -1.0	58 bulan	20.14%

Table 3 indicates that wet/normal conditions dominate (~52%), yet severe drought (~20%) remains hydrologically significant, implying a stable baseline with elevated extreme-event probability. Hence, drought risk cannot be represented by mean conditions alone but requires probabilistic characterization. Persistence is further evaluated via event duration in Table 4.

Table 4. Drought event duration characteristics based on SPI during 2001-2024

Parameter	Value	Interpretation
Number of drought events	25	Occurrence frequency of drought events

Nusantara Hasana Journal
Volume 3 No. 7 (Desember 2023), Page: 236-248
E-ISSN : 2798-1428

Total drought months	88	Cumulative drought months during the study period
Maximum duration	6 months	Longest continuous drought episode
Minimum duration	1 month	Shortest drought episode
Average duration	3.52 months	Average persistence of drought events
Most severe SPI	-2.19	Most severe drought anomaly

Maximum drought duration and average event duration indicate that drought in the Jeneberang Basin is not merely transient but can persist across multiple consecutive months, thereby amplifying cumulative rainfall deficits. Although the rainfall trend analysis in Subsection 3.1 indicates no statistically significant long-term trend, the SPI-based event analysis reveals recurrent dry anomalies with measurable intensity, frequency, and persistence. Therefore, based on Figure 3, Table 3, and Table 4, SPI(t) provides a probabilistic representation of drought variability and serves as a key control variable for adaptive water allocation.

Dataset Validation (Error and Consistency Analysis)

Rainfall data reliability is assessed through cross-validation between CHIRPS (primary dataset) and NASA POWER (benchmark). Performance is evaluated using error metrics (RMSE, MAE, bias) and statistical consistency indicators (R, R^2, p-value). The validation results are presented in Figure 4. Which is figure 4(a) shows strong linear agreement between CHIRPS and NASA POWER (R=0.946), indicating consistent representation of rainfall variability, although deviations from the 1:1 line reveal magnitude discrepancies. Figure 4(b) confirms temporal pattern consistency, while Figure 4(c) indicates a systematic negative bias, implying CHIRPS tends to estimate higher rainfall than NASA POWER. These findings are further quantified in Table 5.

Table 5. Consistency and error evaluation between CHIRPS and NASA POWER datasets

Parameter	Value	Interpretation
Observation Period	2001-2024	Analysis timeframe
Number of Data	288 months	Time series length
RMSE	136.76 mm	Moderate total deviation
MAE	92.94 mm	Moderate absolute error
Bias	-88.53 mm	CHIRPS tends to overestimate rainfall
Correlation Coefficient (R)	0.946	Very strong consistency
Coefficient of Determination (R^2)	0.894	Very high explained variance
p-value	0.0000	Statistically significant relationship
Regression Model	NASA = 2.07 + 0.66 × CHIRPS	Linear inter-dataset relationship

Nusantara Hasana Journal
Volume 3 No. 7 (Desember 2023), Page: 236-248
E-ISSN : 2798-1428

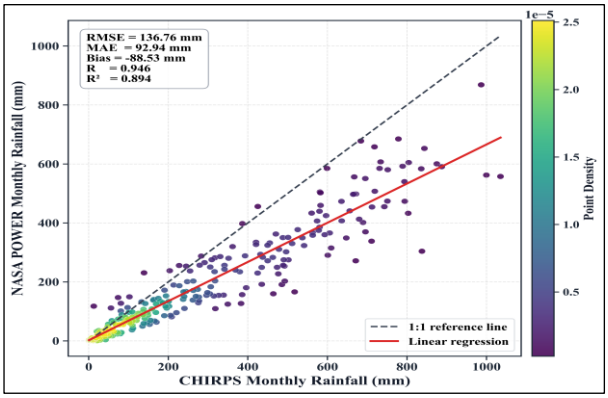

(a)

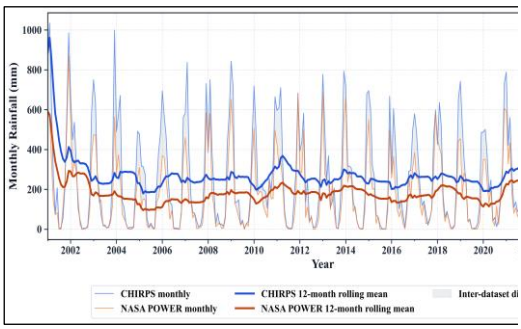

(b)

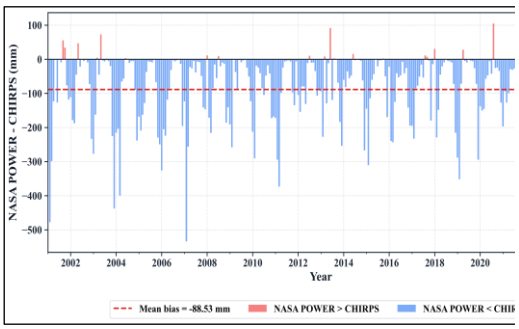

(c)

Figure 4. (a) Cross-dataset rainfall agreement, (b) monthly rainfall time series comparison, (c) monthly difference and bias pattern

$R^2 = 0.894$ indicates strong inter-dataset consistency, while elevated RMSE and MAE suggest scaling bias under high rainfall conditions. Overall, CHIRPS is suitable for SPI(t)-based anomaly analysis but requires caution for extreme events.

Evaluation Baseline

To assess initial performance, a static water allocation model is evaluated as a baseline, assuming time-invariant hydrological conditions and ignoring temporal variability. The baseline results are summarized in Table 6.

Table 6. Performance of the baseline water allocation model

Parameter	Value	Interpretation
Total Demand	86,400	Total system requirement
Total Effective Supply	46,612.88	Actual available water
Total Allocation	40,021.62	Successfully allocated water
Total Deficit ((D_{base}))	46,378.38	Significant water shortage
Deficit Ratio (%)	53.68	More than half of demand unmet
System Efficiency (%)	46.32	Low allocation efficiency

Table 6 indicates severe baseline underperformance, with a 53.68% deficit and 46.32% efficiency caused by temporally static allocation. Therefore, SPI(t)-based adaptive allocation is introduced, as presented in Figure 5 and Table 7.

Nusantara Hasana Journal
Volume 3 No. 7 (Desember 2023), Page: 236-248
E-ISSN : 2798-1428

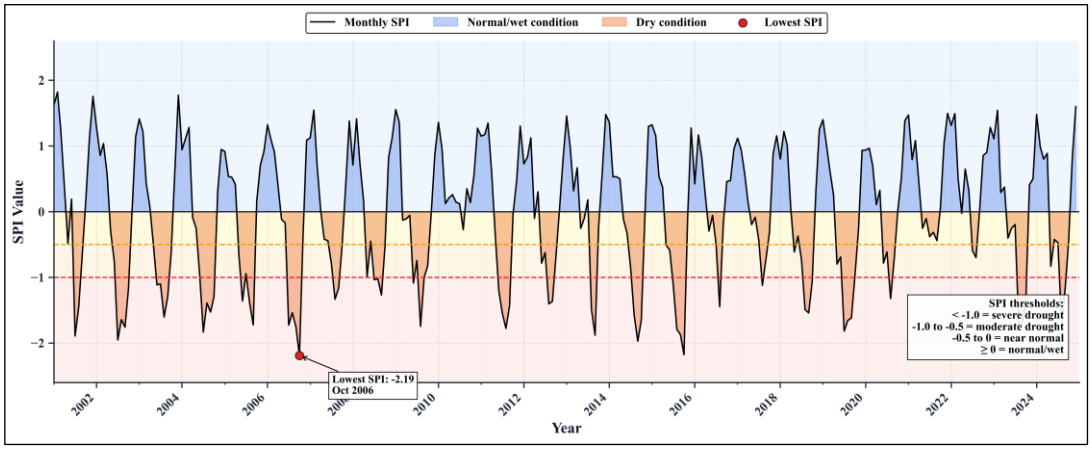

(a)

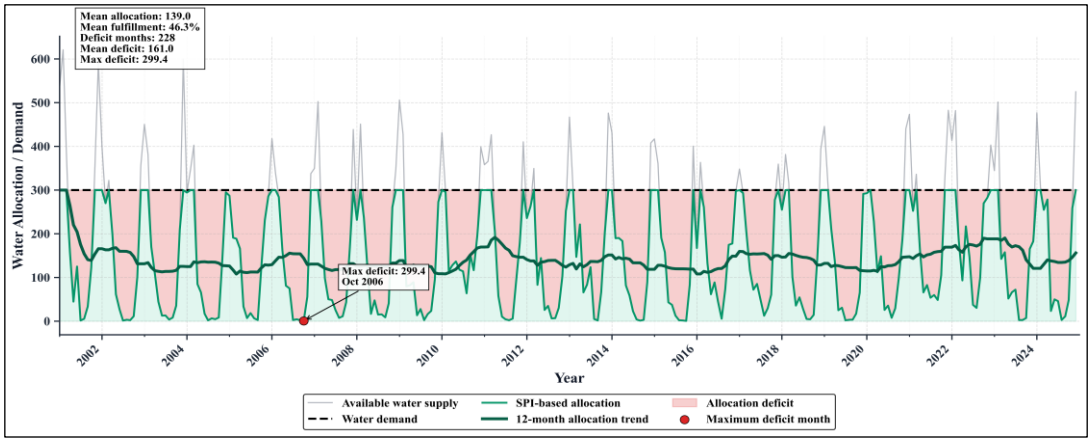

(b)

Figure 5. (a) Temporal SPI dynamics and (b) water allocation response to hydrological variability

Table 7. Performance improvement of the SPI-based allocation model vs. baseline

Parameter	Value	Interpretation
Total Adjusted Demand	86,796.21	Dynamic demand
Total Adjusted Supply	57,620.93	SPI-adaptive supply
Total Allocation (Model)	46,426.17	More optimal distribution
Total Deficit ((D_{model}))	40,370.04	Significant reduction
Deficit Ratio (%)	46.51	Reduced risk
System Efficiency (%)	53.49	Improved efficiency

Figure 5 and Table 7 show that SPI(t)-driven adaptive allocation reduces temporal mismatch, lowering deficit and improving efficiency through dynamic state-based control of W(t). Further temporal and cumulative comparisons are presented in Figure 6 and Table 8.

Nusantara Hasana Journal
Volume 3 No. 7 (Desember 2023), Page: 236-248
E-ISSN : 2798-1428

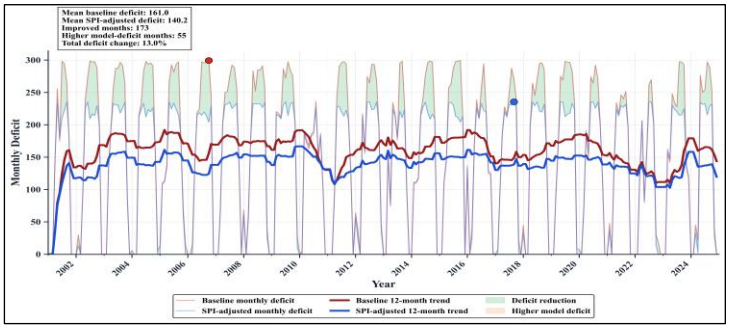

(a)

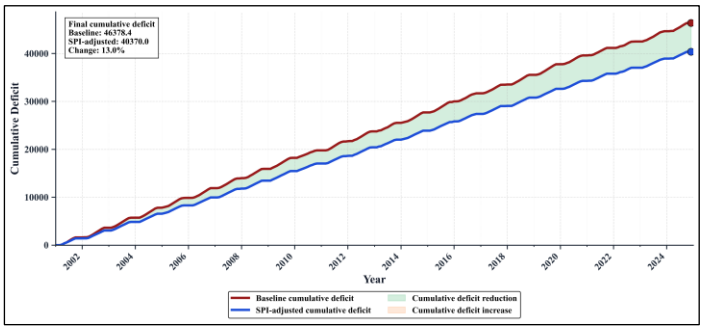

(b)

Figure 6. (a) Temporal deficit comparison and (b) cumulative deficit comparison

Table 8. Performance improvement of the SPI-based model vs. baseline

Parameter	Value
Baseline Deficit	46,378.38
Model Deficit	40,370.04
Absolut Deficit Reduction	6,008.34
Deficit Reduction (%)	12.96

Figure 6(a) shows consistently lower deficits under the SPI-based model, while Figure 6(b) indicates slower cumulative growth, reflecting improved long-term efficiency. Table 8 confirms a 12.96% reduction. Analytically, this gain arises from SPI(t)-driven adaptation that reduces supply-demand mismatch, transforming allocation from static to adaptive.

Sensitivity Analysis

Model robustness is evaluated via sensitivity of $A(t)$to $SPI(t)$. The relationship is shown in Figure 7, with quantitative metrics summarized in Table 9.

Nusantara Hasana Journal
Volume 3 No. 7 (Desember 2023), Page: 236-248
E-ISSN : 2798-1428

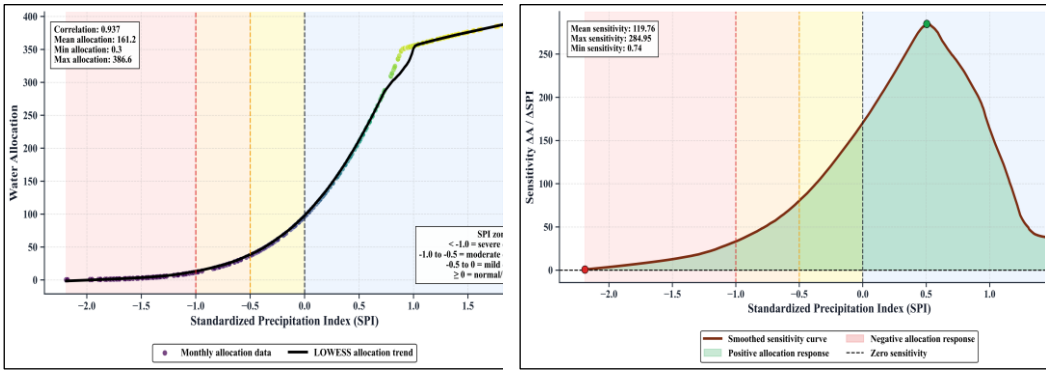

(a) **(b)**

Figure 7. (a) SPI-allocation relationship and (b) allocation sensitivity to SPI

Table 9. Sensitivity of the allocation model to SPI variations

Component	Value
Mean	117.2783
Max	415.0717
Std	115.3981
Normal Range	171.1173
Extreme Range	25.3647

Figure 7(a) shows a non-linear, continuous, and strongly correlated $SPI(t) - A(t)$ relationship, indicating stable coupling without discontinuity. Figure 7(b) and Table 9 reveal non-uniform sensitivity: mean = 117, higher in normal range (171) than extreme (25), reflecting bounded responsiveness—adaptive under typical conditions but constrained under extremes, preventing overreaction while maintaining allocation stability.

CONCLUSION

This study proposes an adaptive water allocation framework based on the pipeline P(t)-SPI(t)-A(t), where SPI(t) functions as a probabilistic control variable representing hydrological states. This integration shifts allocation from static, mean-based assumptions to a dynamic, state-driven system. Quantitatively, the model reduces deficit by 12.96% and improves efficiency from 46.32% to 53.49%, confirming that hydrologically adaptive allocation mitigates temporal supply-demand mismatch inherent in static models.

Cross-validation between CHIRPS and NASA POWER demonstrates strong consistency, supporting data reliability, while sensitivity analysis reveals bounded responsiveness—adaptive under normal conditions and stable under extremes. Conceptually, the key contribution lies in reformulating $SPI(t)$from a descriptive indicator into a decision variable that establishes an explicit causal link between hydrological conditions and allocation decisions, enhancing both efficiency and system resilience.

However, limitations remain in satellite data uncertainty propagation, distributional assumptions in $SPI(t)$, and simplified supply-demand representation, which may affect absolute accuracy and generalizability. Future work should

Nusantara Hasana Journal
Volume 3 No. 7 (Desember 2023), Page: 236-248
E-ISSN : 2798-1428

integrate machine learning or deep learning-based forecasting to predict $SPI(t)$, enabling a transition from reactive to predictive systems. Additionally, multi-basin validation and real-time decision support integration are required to improve transferability and operational applicability. This study delivers both quantitative performance gains and a conceptual advancement in adaptive water allocation, providing a probabilistic, hydrology-driven framework with strong potential for predictive and real-world implementation.

REFERENCE

1. Dai, M., Huang, S., Huang, Q., Leng, G., Guo, Y., Wang, L., Fang, W., Li, P., & Zheng, X. (2020). Assessing agricultural drought risk and its dynamic evolution characteristics. Agricultural Water Management, 231, 106003. https://doi.org/10.1016/j.agwat.2020.106003
2. Dai, M., Huang, S., Huang, Q., Zheng, X., Su, X., Leng, G., Li, Z., Guo, Y., Fang, W., & Liu, Y. (2022). Propagation characteristics and mechanism from meteorological to agricultural drought in various seasons. Journal of Hydrology, 610, 127897. https://doi.org/10.1016/j.jhydrol.2022.127897
3. Fawen, L., Manjing, Z., Yong, Z., & Rengui, J. (2023). Influence of irrigation and groundwater on the propagation of meteorological drought to agricultural drought. Agricultural Water Management, 277, 108099. https://doi.org/10.1016/j.agwat.2022.108099
4. Guillory, L., Pudmenzky, C., Nguyen-Huy, T., Cobon, D., & Stone, R. (2023). A drought monitor for Australia. Environmental Modelling & Software, 170, 105852. https://doi.org/10.1016/j.envsoft.2023.105852
5. Guo, Y., Huang, S., Huang, Q., Leng, G., Fang, W., Wang, L., & Wang, H. (2020). Propagation thresholds of meteorological drought for triggering hydrological drought at various levels. Science of The Total Environment, 712, 136502. https://doi.org/10.1016/j.scitotenv.2020.136502
6. Jehanzaib, M., Shah, S. A., Yoo, J., & Kim, T.-W. (2020). Investigating the impacts of climate change and human activities on hydrological drought using non-stationary approaches. Journal of Hydrology, 588, 125052. https://doi.org/10.1016/j.jhydrol.2020.125052
7. Li, Q., He, P., He, Y., Han, X., Zeng, T., Lu, G., & Wang, H. (2020). Investigation to the relation between meteorological drought and hydrological drought in the upper Shaying River Basin using wavelet analysis. Atmospheric Research, 234, 104743. https://doi.org/10.1016/j.atmosres.2019.104743
8. Noorisameleh, Z., Khaledi, S., Shakiba, A., Firouzabadi, P. Z., Gough, W. A., & Qader Mirza, M. M. (2020). Comparative evaluation of impacts of climate change and droughts on river flow vulnerability in Iran. Water Science and Engineering, 13(4), 265-274. https://doi.org/10.1016/j.wse.2020.05.001
9. Raposo, V. de M. B., Costa, V. A. F., & Rodrigues, A. F. (2023). A review of recent developments on drought characterization, propagation, and influential factors. Science of The Total Environment, 898, 165550. https://doi.org/10.1016/j.scitotenv.2023.165550
10. Shao, S., Zhang, H., Singh, V. P., Ding, H., Zhang, J., & Wu, Y. (2022). Nonstationary analysis of hydrological drought index in a coupled human-water system: Application of the GAMLSS with meteorological and

Nusantara Hasana Journal
Volume 3 No. 7 (Desember 2023), Page: 236-248
E-ISSN : 2798-1428

anthropogenic covariates in the Wuding River basin, China. Journal of Hydrology, 608, 127692. https://doi.org/10.1016/j.jhydrol.2022.127692

11. Sun, P., Liu, R., Yao, R., Shen, H., & Bian, Y. (2023). Responses of agricultural drought to meteorological drought under different climatic zones and vegetation types. Journal of Hydrology, 619, 129305. https://doi.org/10.1016/j.jhydrol.2023.129305
12. Sun, P., Ma, Z., Zhang, Q., Singh, V. P., & Xu, C.-Y. (2022). Modified drought severity index: Model improvement and its application in drought monitoring in China. Journal of Hydrology, 612, 128097. https://doi.org/10.1016/j.jhydrol.2022.128097
13. Tramblay, Y., Koutroulis, A., Samaniego, L., Vicente-Serrano, S. M., Volaire, F., Boone, A., Le Page, M., Llasat, M. C., Albergel, C., Burak, S., Cailleret, M., Kalin, K. C., Davi, H., Dupuy, J.-L., Greve, P., Grillakis, M., Hanich, L., Jarlan, L., Martin-StPaul, N., … Polcher, J. (2020). Challenges for drought assessment in the Mediterranean region under future climate scenarios. Earth-Science Reviews, 210, 103348. https://doi.org/10.1016/j.earscirev.2020.103348
14. Wang, F., Wang, Z., Yang, H., Di, D., Zhao, Y., Liang, Q., & Hussain, Z. (2020). Comprehensive evaluation of hydrological drought and its relationships with meteorological drought in the Yellow River basin, China. Journal of Hydrology, 584, 124751. https://doi.org/10.1016/j.jhydrol.2020.124751
15. Wu, Y., Gan, T. Y., She, Y., Xu, C., & Yan, H. (2020). Five centuries of reconstructed streamflow in Athabasca River Basin, Canada: Non-stationarity and teleconnection to climate patterns. Science of The Total Environment, 746, 141330. https://doi.org/10.1016/j.scitotenv.2020.141330
16. Yang, B., Cui, Q., Meng, Y., Zhang, Z., Hong, Z., Hu, F., Li, J., Tao, C., Wang, Z., & Zhang, W. (2023). Combined multivariate drought index for drought assessment in China from 2003 to 2020. Agricultural Water Management, 281, 108241. https://doi.org/10.1016/j.agwat.2023.108241
17. Zhang, X., Hao, Z., Singh, V. P., Zhang, Y., Feng, S., Xu, Y., & Hao, F. (2022). Drought propagation under global warming: Characteristics, approaches, processes, and controlling factors. Science of The Total Environment, 838, 156021. https://doi.org/10.1016/j.scitotenv.2022.156021